Available online at www.sciencedirect.com
ScienceDirect
Developmental Biology 311 (2007) 487–499
DEVELOPMENTAL BIOLOGY
www.elsevier.com/developmentalbiology

The *Drosophila* Dead end Arf-like3 GTPase controls vesicle trafficking during tracheal fusion cell morphogenesis

Lan Jiang [a,b,d], Stephen L. Rogers [b,c], Stephen T. Crews [a,b,d,*]

[a] *Department of Biochemistry and Biophysics, The University of North Carolina at Chapel Hill, Chapel Hill, NC 27599-3280, USA*
[b] *Department of Biology, The University of North Carolina at Chapel Hill, Chapel Hill, NC 27599-3280, USA*
[c] *Carolina Center for Genome Sciences, The University of North Carolina at Chapel Hill, Chapel Hill, NC 27599-3280, USA*
[d] *Program in Molecular Biology and Biotechnology, The University of North Carolina at Chapel Hill, Chapel Hill, NC 27599-3280, USA*

Received for publication 17 July 2007; revised 24 August 2007; accepted 28 August 2007
Available online 7 September 2007

Abstract

The *Drosophila* larval tracheal system consists of a highly branched tubular organ that becomes interconnected by migration-fusion events during embryonic development. Fusion cells at the tip of each branch guide migration, adhere, and then undergo extensive remodeling as the tracheal lumen extends between the two branches. The *Drosophila dead end* gene is expressed in fusion cells, and encodes an Arf-like3 GTPase. Analyses of *dead end* RNAi and mutant embryos reveal that the lumen fails to connect between the two branches. Expression of a constitutively active form of Dead end in S2 cells reveals that it influences the state of actin polymerization, and is present on particles that traffic along actin/microtubule-containing processes. Imaging experiments in vivo reveal that Dead end-containing vesicles are associated with recycling endosomes and the exocyst, and control exocyst localization in fusion cells. These results indicate that the Dead end GTPase plays an important role in trafficking membrane components involved in tracheal fusion cell morphogenesis and lumenal development.

Keywords: Arf-like GTPase; Arf-like3; *CG6560*; *Dead end*; *Drosophila*; Exocyst; Fusion; GTPase; Trachea

Introduction

The insect trachea is a highly branched tubular network that delivers oxygen throughout the body (Manning and Krasnow, 1993). Segmentally repeated groups of tracheal precursor cells extend branches during embryonic development. Most of these branches are led in their migration by specialized fusion or tip cells (Samakovlis et al., 1996a,b; Tanaka-Matakatsu et al., 1996). The migrating fusion cells recognize and adhere to each other via filopodial extensions. After the fusion cells join, Shotgun (Shg; *Drosophila* DE-cadherin) accumulates at the fusion site (Tanaka-Matakatsu et al., 1996) and initiates the formation of a Short Stop/actin/microtubule-containing track that extends through the cell and acts as a template for the deposition of membrane and lumenal components (Lee and Kolodziej, 2002). Ultimately, the lumen extends between fusion cells and joins to the lumen from adjacent non-fusion tracheal cells to form a continuous tube. Simultaneously, the fusion cell soma is displaced asymmetrically around the lumen, the cells are sealed by adherens junctions, and the fusion cells take on a doughnut-shaped appearance. These processes require a well-coordinated variety of cytoskeletal rearrangements and cell shape changes involving membrane assembly events (Hogan and Kolodziej, 2002).

Trafficking of components to the membrane can occur by a: (1) direct endoplasmic reticulum to Golgi to membrane pathway, or (2) recycling endosome pathway. Transport to the plasma membrane from the Golgi involves vesicle transport and can be either unregulated or require the release of stored secretory

* Corresponding author. Department of Biochemistry and Biophysics, The University of North Carolina at Chapel Hill, Chapel Hill, NC 27599-3280, USA. Fax: +1 919 962 4296.
E-mail address: steve_crews@unc.edu (S.T. Crews).

0012-1606/$ - see front matter © 2007 Elsevier Inc. All rights reserved.
doi:10.1016/j.ydbio.2007.08.049

vesicles by a regulated stimulus. Membrane components can also be endocytosed and recycled back to the membrane via recycling endosomes. In both cases, transport of vesicles to the membrane may require trafficking along microtubules and actin networks (Wang and Hsu, 2006). In some cases, vesicle trafficking to the membrane requires the exocyst, a conserved complex of 8 proteins (Sec3, Sec5, Sec6, Sec8, Sec10, Sec15, Exo70, and Exo84), which can direct specific proteins for exocytosis to preferred sites in the membrane. Numerous functions of the exocyst exist. They include the control of vesicle trafficking along microtubule and actin cytoskeletal elements, regulation of protein synthesis, and docking of secretory vesicles to the plasma membrane (Wang and Hsu, 2006). In *Drosophila*, the exocyst was shown to direct: (1) Shg from recycling endosomes to the adherens junction in the thoracic epithelium (Langevin et al., 2005), (2) Gurken to specific sites in the oocyte membrane for signaling to follicle cells (Murthy and Schwarz, 2004), (3) endocytic recycling of the Yolkless vitellogenin receptor via coated pits (Sommer et al., 2005), and (4) neurite extension (Murthy et al., 2003). In addition, there are examples where exocyst function is influenced by interactions with GTPases (Wang and Hsu, 2006). Thus, the exocyst is versatile and regulated, yet it shows specificity since it is not required for all membrane trafficking events.

One of the key questions of tracheal development is what controls the multiple morphogenetic events that occur during tracheal fusion? In this paper, we describe the *dead end* (*dnd*) Arf-like3 (Arl3) GTPase gene, which is expressed in tracheal fusion cells. *dnd* is required for proper lumenal fusion in the tracheal dorsal branch (DB) and dorsal trunk (DT). Experiments in *Drosophila* S2 cells showed that activated *dnd* resulted in loss of F-actin polymer, and Dnd protein was associated with particles that track on actin/microtubule-containing processes. The Dnd^{+} particles were also associated with components of recycling endosomes and the exocyst. This observation led to further experiments examining fusion cells, and a population of Dnd^{+} vesicles was observed to overlap with Sec5 and Rab11, which are protein components of the exocyst and recycling endosomes, respectively. These vesicles accumulate around the fusion site, and *dnd* is required for fusion cell localization of Sec5. These results indicate that Dnd directs trafficking of vesicles to fusion cell membranes, and is required for formation of a continuous lumen.

Materials and methods

Drosophila strains

Drosophila strains included the *dnd P*-element mutant, *P{XP} CG6678^{d10234}/TM3*, *dnd* deletion strain, *Df(3R)Exel6188* [93F8-14], and *sec5* mutants: *sec5^{E10}* and *sec5^{E13}* (Murthy et al., 2003). *Gal4* lines employed to express *UAS* transgenes were: *breathless* (*btl*)-*Gal4* (all tracheal cells) and *escargot-Gal4* (fusion cells) (Jiang and Crews, 2006). *UAS* lines included: *UAS-GFP-actin* (Jiang and Crews, 2006), *UAS-GFP-Gap43* (Lee et al., 2003), *UAS-GFP-Rab5/CyO* (Shimizu et al., 2003), *UAS-GFP-Rab7* (Entchev et al., 2000), *UAS-GFP-Rab11* (Satoh et al., 2005), and *UAS-CFP-Golgi* (Satoh et al., 2005). *dnd* was balanced over *TM3 twist-Gal4 UAS-GFP*, and homozygous mutant embryos were identified by their absence of *GFP* expression.

Mutagenesis of the dnd cDNA clone

The coding region of the RE02160 full-length *dnd* cDNA clone (Open Biosystems) was PCR-amplified using the primer pair: 5′-GAATTCATGG-GTCTGCTATCGCTGTTG-3′ and 5′-GAATTCTTACTTCTTCATATTCTTG-CAGACCCA-3′ (*Eco*RI sites are underlined). This fragment was cloned into the *Eco*RI site of pCR-Blunt II-TOPO (Invitrogen), and mutant variants of the *dnd* cDNA (G2A, T31N, and Q71L) were created using the QuikChange II XL site-directed mutagenesis kit (Stratagene).

Dnd antisera

Polyclonal antibodies against Dnd were generated by injecting rats and guinea pigs (Pocono Rabbit Farm and Laboratory Inc.) with an N-terminal 6xHis-tagged Dnd fusion protein. PCR was used to generate a *dnd* cDNA fragment corresponding to amino acids 38–179. This fragment was cloned into the *Nde*I–*Bam*H1 sites of pET-15b (Novagen). After transformation into *E. coli* BL21 (DE3), 6xHis-Dnd protein synthesis was induced by IPTG. Inclusion bodies were isolated, solubilized in 10% SDS, followed by sequential dialysis in: (1) 0.05% SDS, 1 mM PMSF, 1× PBS, (2) 0.01% SDS, 1 mM PMSF, 1× PBS, and (3) 1× PBS.

Drosophila embryo immunostaining

Whole-mount embryos were immunostained using standard techniques (Patel et al., 1987). The following primary antibodies were used for embryonic and S2 cell staining: rat anti-Dysfusion (Dys) (1:200) (Jiang and Crews, 2003), monoclonal antibody (mAb) 2A12 (1:10) (Developmental Studies Hybridoma Bank; DSHB), mAb rat anti-Shg (1:50) (DSHB), rabbit anti-GFP (1:1000; Abcam), rabbit anti-Rab11 (1:1000) (Li et al., 2007), guinea pig anti-Dnd (1:200), mAb anti-Sec5 (1:50) (Murthy et al., 2003), and anti-α-tubulin (1:100; Sigma). The following secondary antibodies were used: Alexafluor 488 anti-guinea pig IgG, Alexafluor 488 anti-rat IgG, Alexafluor 488 anti-rabbit IgG, Alexafluor 546 anti-rat IgG, Alexafluor 594 anti-mouse IgM, and Alexafluor 647 anti-mouse IgG. All secondary antibodies were used at 1:200 dilution except for Alexafluor 594 anti-mouse IgM, which was used at 1:1000. Immunostaining was visualized using a Zeiss Pascal confocal microscope.

dnd RNAi

The embryonic function of *dnd* was analyzed after injections of *dnd* RNAi as previously described (Jiang and Crews, 2003). *GFP* RNAi acted as a negative control (Jiang and Crews, 2003). The DNA templates used for RNAi were the products of two-step PCR. The first step involved PCR generation of a *dnd* cDNA fragment containing a partial T7 RNA polymerase promoter at both ends. The second PCR amplified the first fragment and resulted in the generation of complete T7 RNA polymerase sites. The first PCR reaction utilized the following primer pair:

5′-CGACTCACTATAGGGATGGGTCTGCTATCGCTGTTG-3′
5′-CGACTCACTATAGGGTTACTTCTTCATATTCTTGCAGACCCA-3′

(partial T7 promoter sequences are underlined). The amplified fragment contained 546 bp of *dnd*, including the entire coding sequence. The second step of the PCR for both templates used the T7 promoter sequence:

ATAGAATTCTCTAGAAGCTTAATACGACTCACTATAGGG

as a primer. This resulted in an amplified fragment with T7 RNA polymerase sites at both ends allowing the simultaneous synthesis of sense and anti-sense RNA. RNAi solutions were injected into the ventral side of the embryo around 30–50% egg length using a Picospritzer III picopump. The injected embryos were incubated at 18 °C for 26 h, and either immunostained (stages 15–16), or further incubated at 25 °C, at which time the tracheal phenotypes of 2nd instar larvae were examined by bright-field microscopy.

Generation of UAS-GFP-dnd and UAS-dnd transgenes

Transgenic *UAS* strains containing complete *dnd* coding sequences with and without GFP tags were generated. The *GFP* cDNA fragment was amplified by PCR using primers:

5′-GAATTCATGGTGAGCAAGGGCGAG-3′ 5′-CTCGAGCTTGTACAGCTCGTCCATGCC-3′

(*Eco*RI and *Xho*I sites are underlined), and then cloned into the *Eco*RI and *Xho*I sites of *pUAST* (Brand and Perrimon, 1993) to generate *pUAST-NGFP*. Fragments containing the complete coding sequence of *dnd*, *dndG2A*, *dndT31N*, and *dndQ71L* were PCR-amplified, cut with *Xba*I and *Xho*I, and cloned into the *Xba*I and *Xho*I sites of *pUAST-NGFP*, resulting in transgenes encoding Dnd proteins with GFP at their N-termini. *UAS-dnd* constructs without a *GFP* tag utilized the same *dnd* and *dnd* mutant fragments cloned into *pUAST*. Transgenic flies were generated by standard germline transformation techniques.

Time-lapse visualization of tracheal migration and fusion

Imaging of tracheal migration and fusion was carried-out by examining wild-type and *dnd* mutant *P[btl-Gal4] P[UAS-GFP-actin]* embryos, in which *GFP-actin* was expressed in the trachea. Embryos were collected at room temperature and dechorionated. They were then mounted on a glass coverslip, and immersed in halocarbon oil 700 (Sigma) on slides containing an oxygen-permeable membrane. GFP fluorescent images were captured on a Zeiss LSM-510 confocal microscope with a 60× oil immersion lens for ~2 h. Typically, projections consisted of 14 1 μm slices captured along the *Z*-axis every 2 min. Movies were assembled from projections using ImageJ software.

Cell culture

Drosophila S2 cells were grown in Schneider's medium as previously described (Rogers et al., 2003). S2 cells were transiently transfected with each *UAS-dnd* or *UAS-GFP-dnd* construct along with *pMT-Gal4*, which drives *Gal4* expression via the metallothionein promoter, using Effectene (Qiagen). Cells were incubated for 48 h, and then 500 μM $CuSO_4$ was added to induce *dnd* gene expression. Six hours later, cells were plated on concanavalin A (con A)-treated cover slips for cellular analysis.

S2 cell staining

S2 cell staining involved rinsing cells in HL3 buffer (70 mM NaCl, 5 mM KCl, 1.5 mM $CaCl_2$, 20 mM $MgCl_2$, 10 mM $NaHCO_3$, 5 mM trehalose, 115 mM sucrose, 5 mM HEPES, pH 7.2) (Stewart et al., 1994) followed by fixation for 10 min in 10% paraformaldehyde in HL3 buffer. The cells were then permeabilized in 0.1% Triton X-100 in PBS (PBT) and stained for F-actin with Alexafluor 546-conjugated phalloidin and for DNA with 0.5 μg/ml DAPI. Immunostaining was then carried-out using standard methods, and cells were mounted in 90% glycerol, 10% borate, pH 9.0, 5% *N*-propyl gallate. Cells were examined with a Zeiss 510 confocal microscope.

Time-lapse visualization of particle trafficking in S2 cells

Cotransfection of 0.5 μg *UAS-GFP-dndQ71L* and 0.5 μg *pMT-Gal4* into S2 cells was performed using Effectene, and after incubation for 48 h, the cells were transferred to con A-coated dishes and *GFP-dndQ71L* expression was induced in 2 ml Schneider's medium containing 500 μM $CuSO_4$ for 6 h. GFP fluorescent images were captured on a Perkin-Elmer-Wallac Ultraview spinning disk microscope with a 60× oil immersion lens every 3 s for 10 min. Either 30 μM colchicine was added to inhibit tubulin polymerization, or 10 nM latrunculin was added to inhibit F-actin polymerization. After incubation with inhibitors for 12 h, microscopic examination was carried out. Movies were assembled using ImageJ software.

Results

dnd is expressed in tracheal fusion cells

The Berkeley *Drosophila* Genome Project gene expression database (Tomancak et al., 2002) was screened for genes potentially expressed in tracheal fusion cells. The *CG6560*/*dnd* gene [93F14] is expressed in a pattern resembling fusion cell expression. This was directly tested by co-localization immunostaining experiments in which whole-mount *Drosophila* embryos were stained with antibodies to both Dnd and Dys (Figs. 1A–C). Dys, which is a basic-helix–loop–helix–PAS transcription factor, stains nuclei of tracheal fusion cells

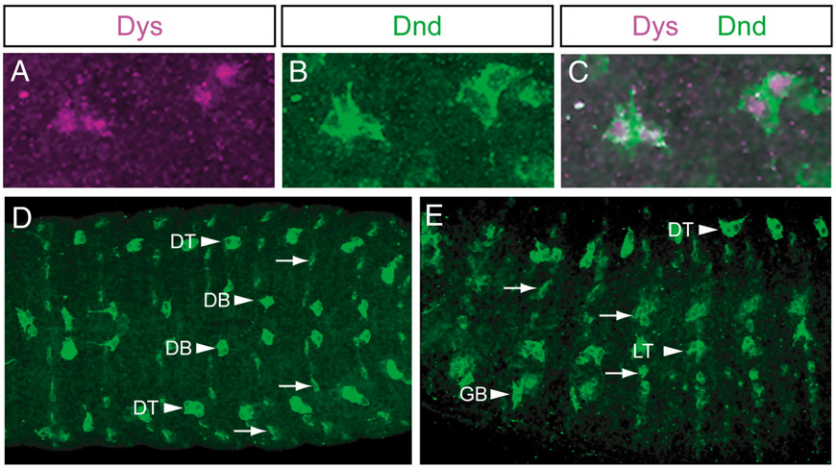

Fig. 1. *dnd* is expressed in embryonic tracheal fusion cells and sensory cells. Whole-mount stage 15 embryos were stained with anti-Dys (A, C; magenta) and anti-Dnd (B–E; green). Anterior is to the left in all panels. (A–C) DT fusion cells show both Dnd (cytoplasmic) and Dys (nuclear) immunoreactivity. Two segments are shown. (D) Dorsal view showing the Dnd^+ fusion cells in segmentally repeated rows of DB and DT tracheal cells (arrowheads). The other Dnd^+ cells are sensory cells (representatives shown by arrows). (E) Sagittal view showing Dnd^+ DT, LT, and GB fusion cells (arrowheads). Dnd^+ sensory cells are indicated by arrows.

(Jiang and Crews, 2003), and overlapped with Dnd reactivity, indicating that *dnd* is expressed in fusion cells. The specificity of Dnd antisera was demonstrated in two ways: (1) the Dnd antisera had the same staining pattern as *dnd* in situ hybridization experiments, and (2) Dnd immunoreactivity was absent in *Df(3R)Exel6188* [93F8-14] homozygous embryos, which delete the *dnd* gene (data not shown). All tracheal fusion cells express *dnd*, including DB, DT, lateral trunk (LT), and ganglionic branch (GB) fusion cells (Figs. 1D–E). *dnd* is also expressed in a subset of embryonic sensory cells (Figs. 1D–E). Subcellular localization of Dnd was throughout the cytoplasm, showing both vesicular and diffuse reactivity (Figs. 1 and 7).

Expression of *dnd* in fusion cells commences at late stage 11 in DT. Expression in LT begins at stage 13, followed by DB and GB expression at stage 14. Expression of *dnd* remains present in fusion cells throughout the remainder of embryonic development. The differences in initiation of *dnd* match the order in which each of the four branch types fuse. DT fusion occurs first (stage 14), followed by LT (stage 15), then DB and GB (stage 16). Sensory cell expression of *dnd* begins at stage 13 and remains on throughout embryogenesis.

dnd encodes a Drosophila Arf-like3 GTPase

The *dnd* gene encodes a 179 aa putative GTPase that most closely resembles Arl3 (Kahn et al., 2006), a protein highly conserved between mammals, *Drosophila*, and *C. elegans*. Dnd is 65% identical to human Arl3 and 55% identical to *C. elegans* arl-3. Alignment of the three proteins is shown Fig. 2A. They share substantial identity and similarity throughout their sequences, and their lengths are similar (179–184 aa). The Dnd sequence is characteristic of GTPases, including a conserved T31 residue, which is required for GTP binding by GTPases, and a Q71 residue, which is normally required for GTP hydrolysis. Both residues have been shown to influence

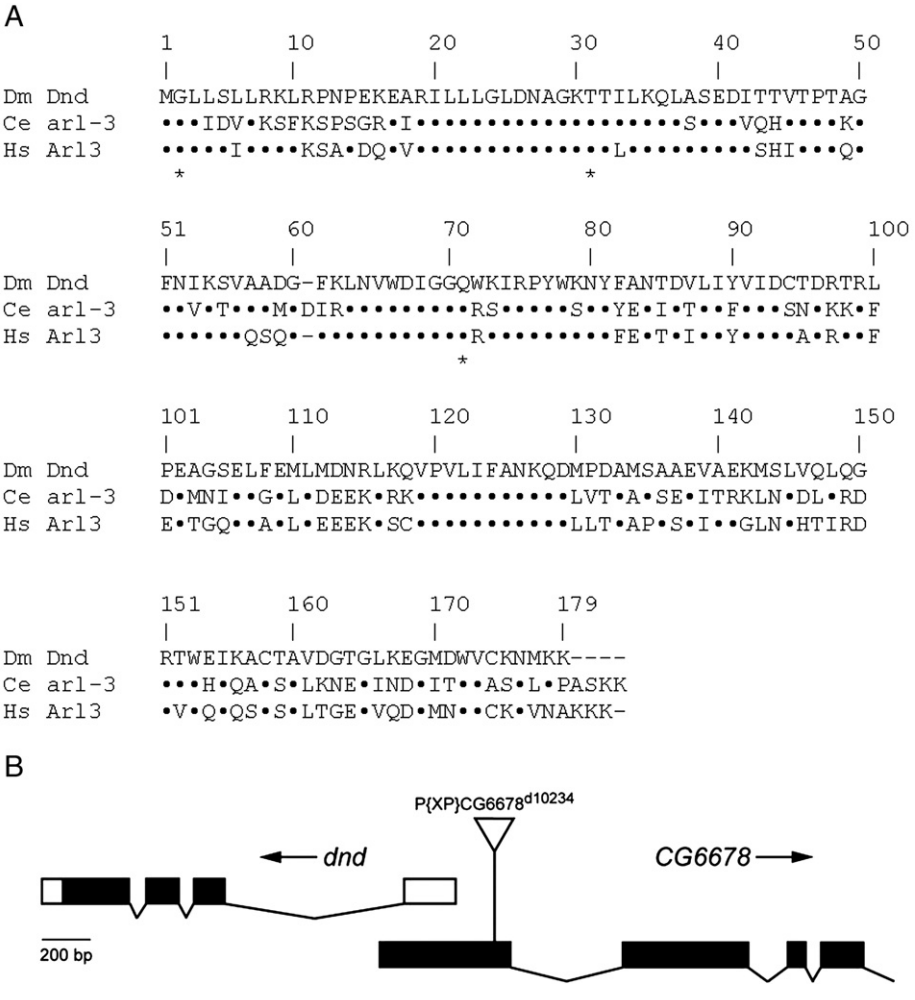

Fig. 2. *dnd* encodes an Arl3 GTPase. (A) Protein sequence alignment of *Drosophila* (Dm) Dnd, and two Arl3 GTPases: *C. elegans* (Ce) arl-3 and human (Hs) Arl3. (●) indicates aa identity. Numbering is at the top based on the *Drosophila* Dnd sequence. Asterisks below the alignment indicate residues putatively required for myristoylation (G2), GTP binding (T31), and GTP hydrolysis (Q71). (B) Genomic organization of the *Drosophila dnd* locus. The intron–exon structure of the *dnd* and *CG6678* genes are shown. *CG6678* is only partially shown and the complete gene spans 20.1 kb. Dark boxes indicate coding sequences and unfilled boxes are untranslated regions. The transcriptional orientations are indicated by arrows. The location of the *P{XP}CG6678^{d010234} P*-element in exon 1 of *CG6678* and in the 5′-flanking sequence of *dnd* is shown. The scale in bp is below the *dnd* schematic.

the biochemical properties of mammalian Arl3 (Linari et al., 1999). In addition, Dnd has G2, which is a myristoylation site in Arf GTPases but this modification has not been observed in Arl3 proteins (Cavenagh et al., 1994). In summary, the sequence of *dnd* suggests that it encodes a functional Arl3 GTPase.

dnd RNAi results in tracheal fusion defects

To initially assess whether *dnd* was required for tracheal development, *dnd* interfering RNA (*dnd* RNAi) was injected into *Drosophila* embryos, and larval trachea examined for evidence of fusion defects. *GFP* interfering RNA (*GFP* RNAi) was employed as a control. Embryos injected with *dnd* RNAi showed an absence of DB fusion in 75% of the segments examined (N=15 embryos and 150 segments scored), whereas control *GFP* RNAi embryos have completely fused trachea in all segments (*N*=10 embryos and 100 segments scored) (Jiang and Crews, 2003) (Figs. 3A, B). In addition, *dnd* RNAi DT tracheal branches were fused, but commonly showed constrictions at the sites of fusion (Figs. 3C, D). LT fusion defects were rare, and GB was not analyzed. Adult viability was also reduced in *dnd* RNAi-injected flies compared to *GFP* RNAi controls. Only 10% (*N*=100 embryos) of *dnd* RNAi embryos hatched into adults compared to 46% (*N*=100 embryos) for *GFP* RNAi-injected embryos. Furthermore, when embryos heterozygous for a deletion of *dnd*, *Df(3R)Exel6188*, were injected with *dnd* RNAi, the frequency of adults was even lower (2%; *N*=100 embryos).

Identification and analysis of a dnd null mutation

While the RNAi data provided evidence that *dnd* is required for proper tracheal formation, it was important to identify a *dnd* mutant for more detailed analyses. The *dnd* gene resides at 93F14 and consists of 4 exons (Fig. 2B). Exon 1 overlaps in the opposite orientation with exon 1 of the *CG6678* gene. There exists a *P*-element, *P{XP}CG6678*^{d10234}, that resides 163 bp 5′ to *dnd*. Analysis of *P{XP}CG6678*^{d10234} homozygous embryos by either *dnd* in situ hybridization or anti-Dnd immunostaining revealed an absence of *dnd* RNA (data not shown) and protein in tracheal fusion cells (Figs. 3I, J), indicating that *P{XP}CG6678*^{d10234} affected *dnd* expression and represented an RNA/protein null mutation. Analysis of tracheal development by staining mutant embryos with mAb 2A12, which stains the tracheal lumen, revealed DB and DT tracheal defects (Figs. 3E–H) similar in frequency to the *dnd* RNAi defects. DB lumenal breaks were observed in 80% of segments (*N*=20 embryos and 200 segments scored), and DT constrictions were observed in 70% of segments (*N*=7 embryos and 63 segments scored).

One concern is that the *P{XP}CG6678*^{d10234} *P*-element insertion also disrupts exon 1 of *CG6778* (Fig. 2B). Thus, while *P{XP}CG6678*^{d10234} is clearly mutant for *dnd*, it could also be mutant for *CG6678*, thereby complicating interpretation of the genetic results. To test whether the *P{XP}CG6678*^{d10234} mutant tracheal phenotype was due to *dnd*, transgenic rescue experiments were performed in *P{XP}CG6678*^{d10234} mutant embryos by expressing wild-type and variant *dnd* genes in fusion cells. The *dnd* variants were G2A, T31N, and Q71L. G2A could disrupt myristoylation and membrane-targeting of *dnd*. T31N is expected to abolish GTP binding, thus yielding an inactive protein. Q71L is predicted to disrupt GTP hydrolysis, resulting in a constitutively-active form of the protein. All were introduced into *Drosophila* as *UAS* transgenes, and expression driven in fusion cells using *escargot-Gal4* (Samakovlis et al., 1996b). Embryos were stained with mAb 2A12, and the number of lumenal breaks was counted. The *dnd* mutant embryos had 20% fused DB. Three of the *dnd* transgenes had high degrees of rescue: unmutated (87% fused DB), Q71L (85% fused), and G2A (79% fused) (100 segments were analyzed for each strain). The putatively inactive T31N strain had a much lower degree of rescue (41% fused DB). These results and other observations strongly support the notion that the tracheal defects observed in *P{XP}CG6678*^{d10234} are due to loss of *dnd* and not *CG6678*: (1) the mutant tracheal defects were closely mimicked by *dnd* RNAi, (2) mutant embryos did not possess any detectable *dnd* RNA or protein, (3) the mutant phenotype was efficiently rescued by expression of wild-type or constitutively-active forms of *dnd* in mutant fusion cells, (4) rescue was significantly less efficient with a form of *dnd* (T31N) predicted to be reduced in GTPase activity, and (5) in situ hybridization of wild-type embryos with a *CG6678* probe failed to detect significant embryonic expression in tracheal or non-tracheal cells (one exception: staining was observed in the salivary gland of late-stage embryos, although this may be artifactual).

dnd mutants have defects in lumen formation

More detailed insight into the role of *dnd* in tracheal development emerged from analysis of *P{XP}CG6678*^{d10234} mutant embryos by time-lapse microscopy. Wild-type and *dnd* mutant trachea were visualized using *UAS-GFP-actin* driven in trachea with *btl-Gal4* (Jiang and Crews, 2006). The *GFP-actin* reporter allows visualization of: (1) fusion cell bodies via cortical actin, (2) filopodial extensions of migrating cells, and (3) the actin surrounding the tracheal lumen. DB development was analyzed since it is easy to visualize migration, adhesion, and fusion, and DB has the most prominent *dnd* mutant tracheal defects. In wild-type trachea over a 2 h period (Figs. 4A–E; Supplemental Movie 1), the fusion cells approached each other with extensive filopodial extensions (Fig. 4A), followed by their mutual adherence (Fig. 4B). The actin-containing lumen emerged in the fusion cells from the side opposite the fusion site, and then progressed toward the site of fusion where it joined with the developing actin-surrounding fusion track. Ultimately, a continuous lumen formed between the two branches (Figs. 4C–E). In the *dnd* mutant, DB migrated normally, extended filopodia, and recognized and adhered to its partner fusion cell (Figs. 4F–G; Supplemental Movie 2). However, unlike wild-type, the tracheal lumen failed to connect between the two fusion cells leaving a gap (Figs. 4H–J). This suggests that *dnd* may be influencing lumen growth at the site of fusion.

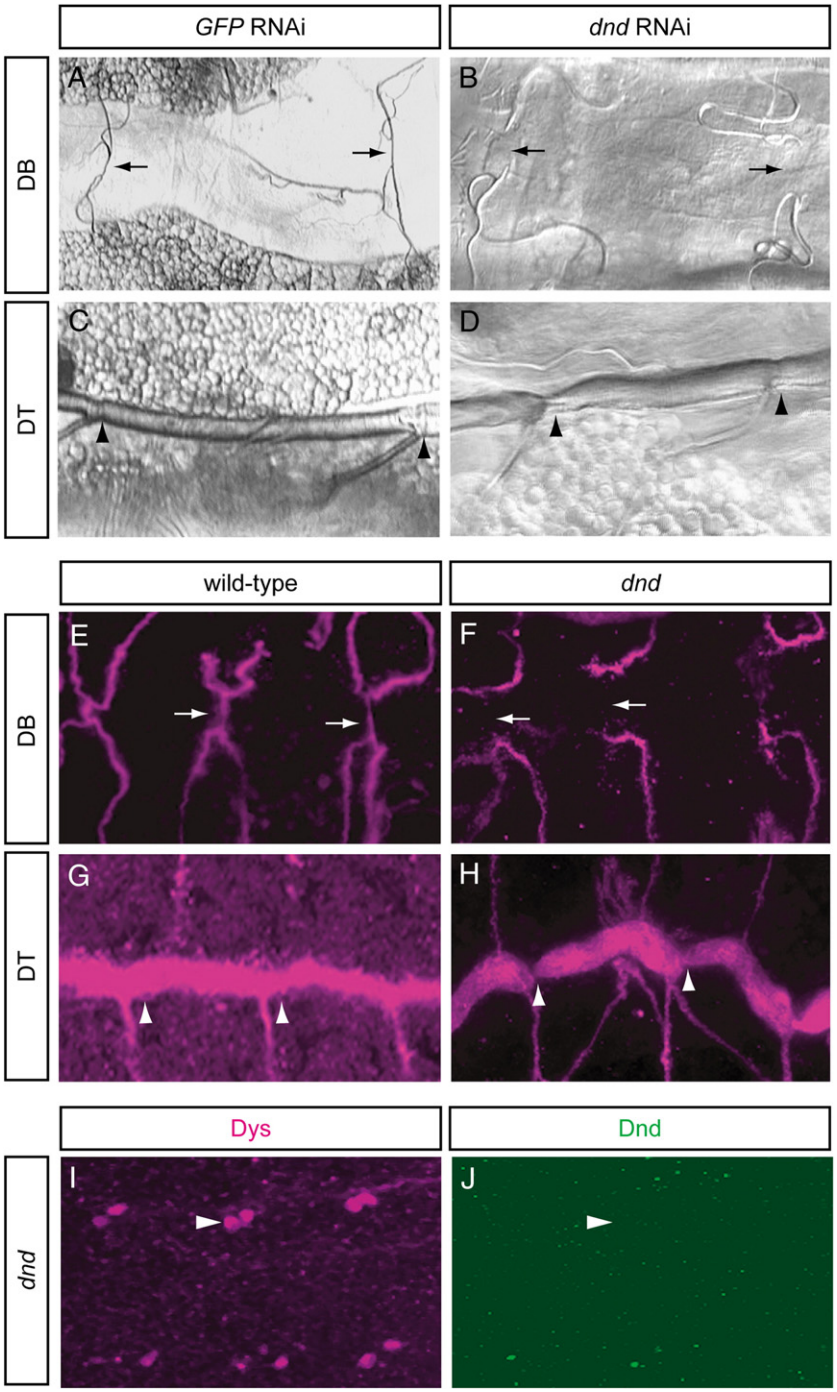

Fig. 3. *dnd* RNAi and *dnd* mutations cause tracheal defects. (A–D) Embryos were injected with either control *GFP* RNAi (A, C) or *dnd* RNAi (B, D), and 2nd instar larvae examined under brightfield microscopy for tracheal defects. (A) Two larval segments showing wild-type-appearing fused DB after injection of *GFP* RNAi. The lumen is continuous between segments. Arrows indicate sites of fusion. (B) DB of *dnd* RNAi-injected larvae showing an absence of a continuous lumen, although branches migrated to the dorsal midline. Arrows mark where lumen fusion normally occurs. (C) DT of *GFP* RNAi-injected embryo showing normal continuous DT lumen. Arrowheads indicate sites of fusion. (D) DT of *dnd* RNAi-injected embryos has a continuous lumen, but with constrictions at sites of fusion (arrowheads). (E–H) Wild-type (E, G) or $P\{XP\}CG6678^{d10234}$ *dnd* mutant (F, H) embryos were examined for tracheal defects by mAb 2A12 staining (magenta). Dorsal views of stage 16 embryos showing: (E) lumenal fusion in wild-type DB (arrows mark fusion sites), and (F) the absence of lumenal fusion in *dnd* mutant DB (arrows indicate where fusion normally occurs). (G, H) Wild-type (G) and *dnd* mutant (H) stage 15 embryos showing lumenal constrictions at fusion sites in mutant DT. Arrowheads indicate sites of fusion. (I, J) Stage 15 *dnd* mutant embryo stained with anti-Dys (I; magenta) and anti-Dnd (J; green) showing the absence of Dnd protein in Dys^{+} fusion cells. Arrowhead shows DT fusion cells.

When activated *dndQ71L* was ectopically expressed throughout the trachea with *btl-Gal4*, ectopic fusion events were observed (Figs. 7A, B). While this is a relatively rare event (1% of segments; $N=1000$ segments scored), it complements the *dnd* mutant results, and reinforces the idea that activated *dnd* controls aspects of tracheal branch fusion.

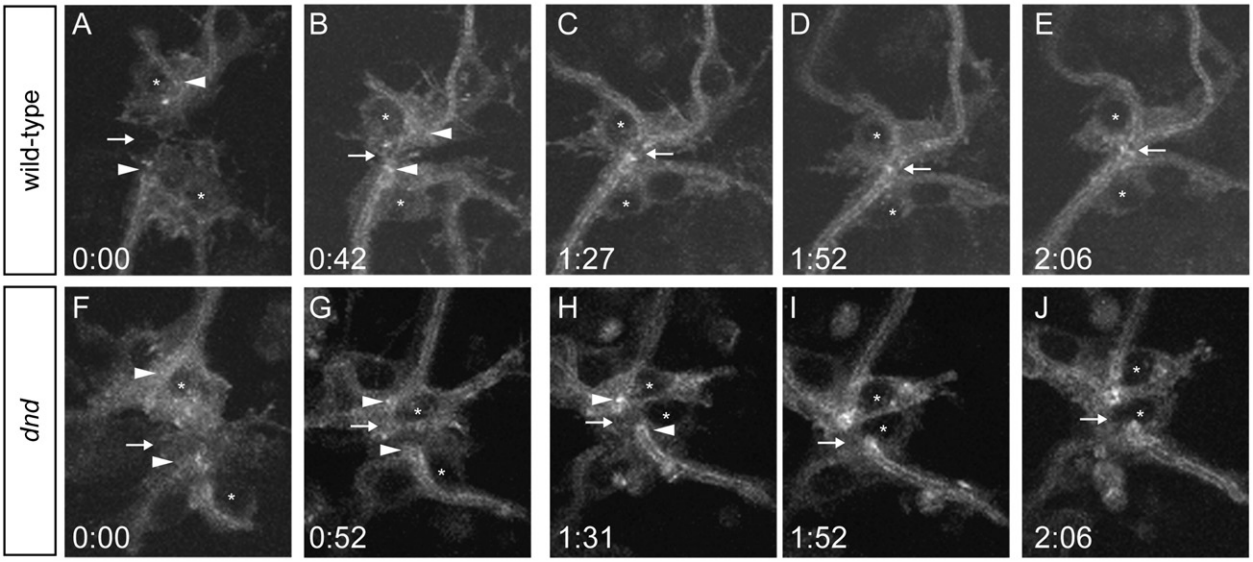

Fig. 4. Time-lapse imaging indicates that *dnd* mutant trachea fail to form a continuous lumen. Development of *btl-Gal4 UAS-GFP-actin* (A–E) wild-type and (F–J) *dnd* mutant trachea were examined live for ~2 h by confocal microscopy. Elapsed times in hours and minutes are shown at the bottom of each panel. (*) Indicates fusion cell nuclei. (A, F) In wild-type (A) and mutant (F) DB, fusion cells approach each other with extensive filopodial projections (arrows). Arrowheads indicate the proximal extent of the lumenal tracks in each fusion cell. (B, G) As the fusion cells adhere, the lumenal tracks (arrowheads) move closer to the fusion site (arrow). (C–J) In wild-type DB (C–E), the lumen forms a continuous track connecting the two tracheal branches (arrow), whereas in *dnd* (H–J) the lumen never forms at the site of fusion.

Activated dnd results in loss of cortical actin and extension of microtubule and actin-containing processes in S2 cells

While analysis of *dnd* function in embryos provides important functional information, additional insight into function can be uncovered by analysis in cultured cells. We employed a *Drosophila* S2 cell line (Rogers et al., 2003) to investigate the role of *dnd* in cellular dynamics. S2 cells do not express *dnd* at detectable levels (Fig. 5C), so the *dnd* cDNA in unmutated and mutated *UAS* versions was transfected into S2 cells along with *pMT-Gal4*, which allows inducible, high-level expression of *UAS* constructs. Transfected cells were plated on con A-treated coverslips, to observe cellular morphology in a flattened form that is double their untreated diameter (Rogers et al., 2003). Con A-treated cells have a well-formed lamella and well-defined cytoskeleton (Figs. 5A–E). Normally, actin is distributed in 3 observable concentric zones: (1) a dense lamellipodial network at the cell periphery, (2) a central, low-density actin region, and (3) a dense region of puncta surrounding the nucleus (Fig. 5A). Microtubules are present in the central domain surrounding the nucleus (Fig. 5B). When cells were transfected with *dndQ71L*, which is expected to exhibit a constitutively-active GTPase activity, a striking change was observed in cellular morphology. In these cells, lamellae were absent. Instead, long actin and microtubule-containing processes emanated from the cell body in a stellate morphology. Furthermore, visualization of Dnd by either anti-Dnd immunostaining (Fig. 5H) or imaging GFP-tagged Dnd (Figs. 6A, B) indicated that Dnd was also present on the processes. Cells transfected with *dndQ71L* had 44% ($N=100$ cells) of cells with the stellate morphology, whereas cells transfected with *dndT31N* had 1% ($N=100$) with stellate morphology, the same as untransfected, control cells. Cells transfected with *dnd* or *dndG2A* showed an intermediate level of stellate morphology (20%, 17%, respectively; $N=100$). In summary, activated *dnd* causes dramatic changes in cellular morphology and cytoskeletal dynamics. The stellate morphology resembles that observed when actin filaments are disrupted by cytochalasin D (Kural et al., 2005), or when *Arp2/3* expression is reduced in S2 cells (Rogers et al., 2003). Arp2/3 nucleates actin filaments promoting the formation of lamella. Conversely, activated *dnd* may be inhibiting actin assembly or promoting disassembly.

Dnd is present in actin/microtubule-associated particles

When S2 cells were transfected with *dndQ71L*, the microtubule/actin processes possessed particles, likely vesicles, that contain Dnd, as well as actin (Figs. 5F–H, J); the presence of tubulin was less apparent. Transfection with *GFP-dndQ71L*, a GFP-tagged version of *dndQ71L*, resulted in a similar transformation of S2 cells to a stellate morphology (45%; $N=100$ cells) as the untagged *dndQ71L* (44%; $N=100$), and allowed live-imaging of Dnd-containing particles. Time-lapse visualization indicated that these particles traffic along the processes (Figs. 6A, B; Supplemental Movies 3 and 4). Kymographic analysis (Figs. 6A, B) indicated that the particles move bidirectionally. When either actin polymerization was inhibited by latrunculin or microtubule polymerization by colchicine, the processes collapsed and vesicular trafficking was abolished (Figs. 6C, D; Supplemental Movies 5 and 6). These results confirmed that the formation of the processes requires polymerized actin and tubulin, and indicated that the particles are associated with Dnd, and require intact actin and microtubule networks for trafficking.

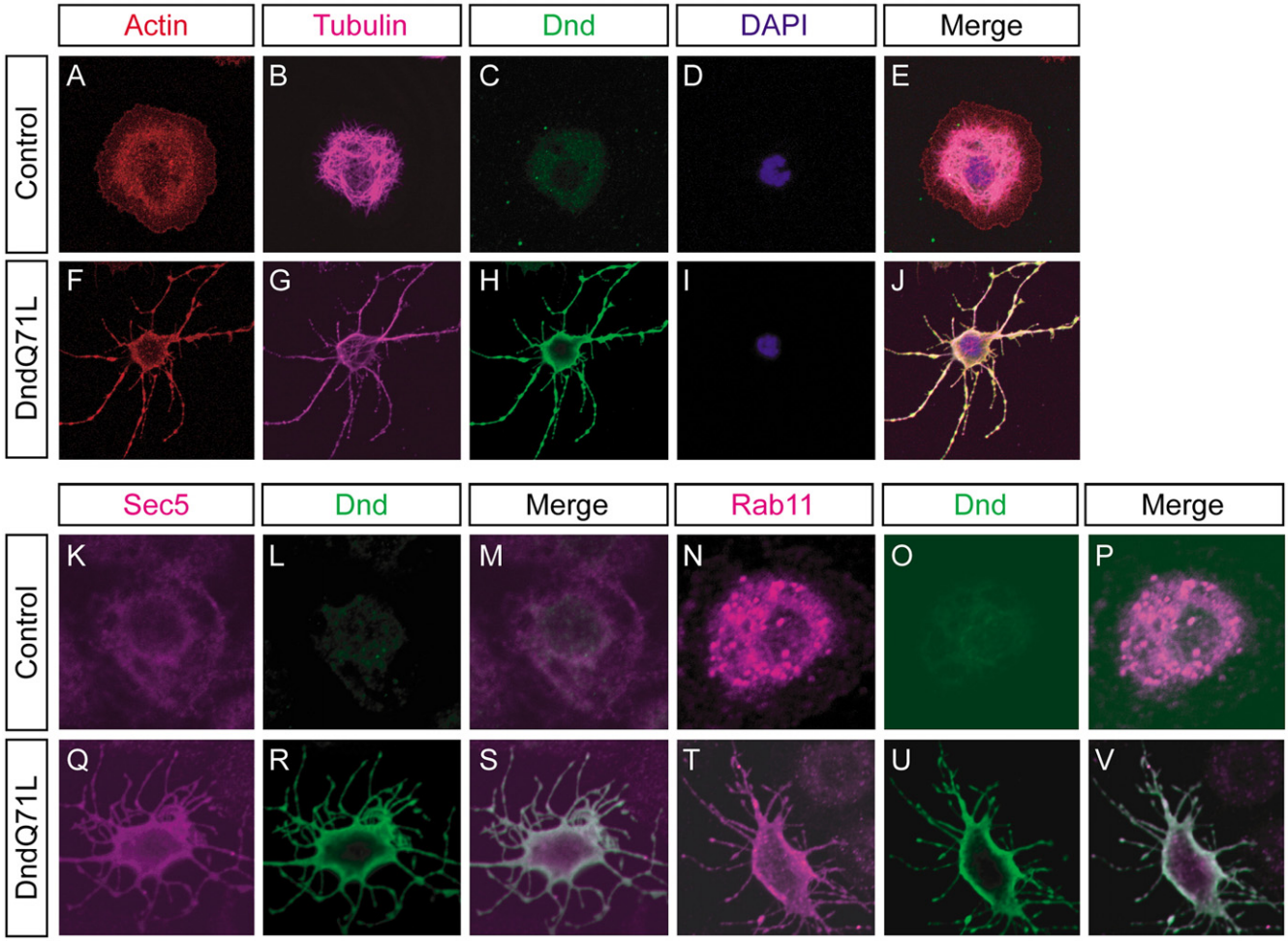

Fig. 5. Activated *dnd* causes cytoskeletal changes in S2 cells. S2 cells either (A–E) untransfected or (F–J) co-transfected with *UAS-dndQ71L* and *pMT-Gal4* and expression induced with $CuSO_4$, were plated on con A-treated coverslips, and stained for (A, F) F-actin (phalloidin, red), (B, G) microtubules (anti-α-tubulin, magenta), (C, H) Dnd (anti-Dnd, green), and (D, I) nuclei (DAPI, blue). (E, J) Merge image. Note the occurrence of actin$^+$ Dnd$^+$ particles along the *dndQ71L*-induced processes. (K–P) Untransfected S2 cells were stained for: (K–M) Sec5 and Dnd, or (N–P) Rab11 and Dnd. (Q–V) S2 cells were transfected with *UAS-dndQ71L* and stained for either (Q–S) Sec5 and Dnd, or (T–V) Rab11 and Dnd. In both cases Sec5$^+$ and Rab 11$^+$ particles overlapped with Dnd$^+$ particles.

Dnd associates with the exocyst and recycling endosomes

The in vivo and cell culture data suggested possible roles for *dnd* in the regulation of: (1) cytoskeletal dynamics and (2) vesicle trafficking to the membrane. Aspects of these events could involve the exocyst, a complex of 8 proteins, including Sec5, which is involved in vesicle trafficking of proteins to the membrane. One aspect of tracheal fusion is the accumulation of Shg at the membrane of the fusion site (Figs. 7C–F) (Lee and Kolodziej, 2002; Tanaka-Matakatsu et al., 1996); a phenomenon that could require Shg$^+$ vesicle trafficking to the membrane. Previously, the *Drosophila* exocyst was shown to control Shg trafficking from recycling endosomes to the membrane in epithelial cells (Langevin et al., 2005). However, *dnd* does not appear to play a major role in this process in fusion cells, since there was substantial localization of Shg at the fusion site in *dnd* mutants (Fig. 7G).

Does Dnd control exocyst function or interact with vesicle trafficking compartments? When trachea were stained for Sec5, the protein was highly enriched at the site of fusion (Fig. 7H), suggesting that the exocyst is delivering vesicles at the site of fusion and membrane reorganization. Consistent with a role in tracheal fusion, *sec5* mutant larvae showed tracheal fusion defects. Both $sec5^{E10}$ and $sec5^{E13}$ mutants (Murthy et al., 2003) showed DB fusion defects resembling *dnd* defects in ~20% DB examined ($sec5^{E10}$: 22% fusion defects; $N=160$ segments scored, and $sec5^{E13}$: 20% fusion defects; $N=100$). Co-staining for Dnd indicated that Dnd was also enriched at the site of fusion, and overlapped with Sec5 (Figs. 7I, J). When Sec5 localization was examined in *dnd* mutant embryos, the enrichment at the fusion site was absent (Figs. 7K–M). Thus, one role of *dnd* may be to promote exocyst-mediated vesicle trafficking to the fusion site membrane. Previous work showed that the exocyst interacts with Rab11$^+$ recycling endosomal vesicles (Langevin et al., 2005). When *GFP-Rab11* was expressed in fusion cells, the recycling endosomal vesicles were found throughout the cell, but some were Dnd$^+$ and found around the fusion site (Figs. 7N–P). Most Dnd$^+$ vesicles were Rab11$^+$. In contrast, Rab7$^+$ late endosomal vesicles (Figs. 7Q–S), Rab5$^+$ early endosomal vesicles (Figs. 7T–V), and Golgi

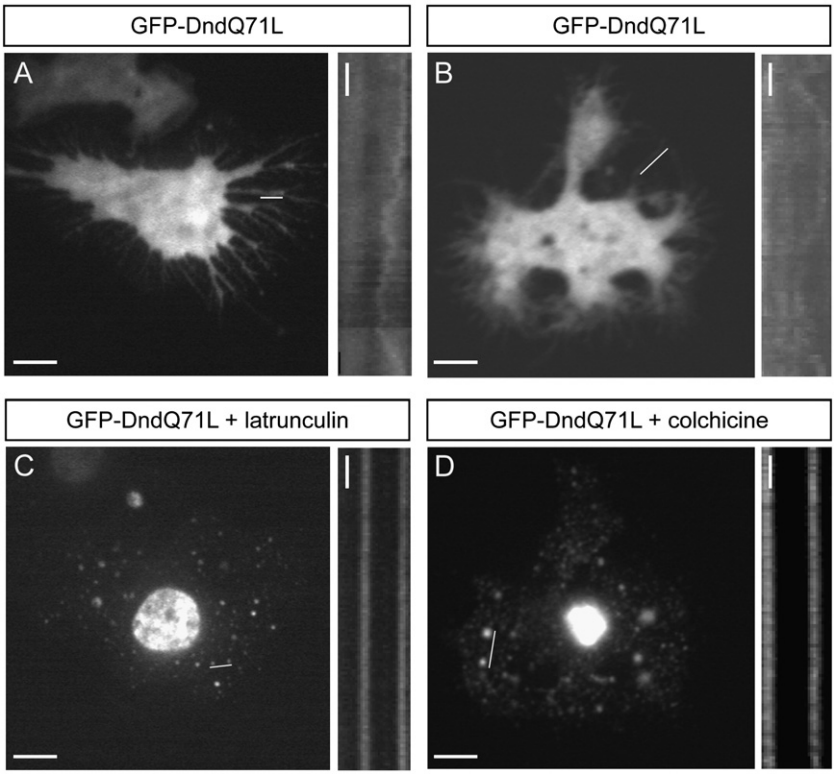

Fig. 6. Trafficking of DndQ71L-containing particles is dependent on both actin and microtubules. S2 cells were transfected with *UAS-GFP-dndQ71L* and *pMT-Gal4* and imaged live for GFP fluorescence. (A, B) Two cells showing the occurrence of GFP-DndQ71L on cellular processes and particles associated with the processes. To the right of each panel is a kymograph of the particles denoted by the line beneath the particles. The vertical line at the top of each kymograph represents a 1 min interval. (A, B) The particles imaged in each kymograph migrate bidirectionally. (C, D) Cells expressing *GFP-dndQ71L* treated with either (C) 10 nM latrunculin to depolymerize actin or (D) 30 μM colchicine to depolymerize tubulin. Treatment resulted in the loss of processes and inhibited particle movement, as demonstrated in the accompanying kymographs. Scale bars = 10 μm.

(Figs. 7W–Y) did not overlap substantially with Dnd^+ vesicles, and their vesicles were not concentrated at the fusion site.

In untransfected S2 cells, Sec5 was found associated with the membrane and as a nuclear annulus (Figs. 5K–M). Previous work showed that some Sec5 was associated with sub-membranous coated pits (Sommer et al., 2005). Rab11 was found in vesicles throughout the cell (Figs. 5N–P). Cells that expressed *dndQ71L* showed that both Sec5 (Figs. 5Q–S) and Rab11 (Figs. 5T–V) were found along the actin/microtubule/Dnd^+ processes. In particular, the Dnd^+ particles found along the processes were also $Sec5^+$ and $Rab11^+$. Thus, similar to the in vivo observations in fusion cells, Dnd, Sec5, and Rab11 overlap in particles that appear to traffic along actin/microtubule-containing tracks. While these particles may or may not be analogous to the Dnd^+ $Sec5^+$ or Dnd^+ $Rab11^+$ vesicles observed in fusion cells, they could provide a useful system for studying a trafficking role of Dnd in cell culture.

Discussion

Dnd is an Arl3 GTPase

Small GTPases are grouped into 5 families: (1) Ras, (2) Rho, (3) Rab, (4) Ran, and (5) Arf. The Arf family can be subdivided into Arf, Sar, and Arl subfamilies (Kahn et al., 2006). Sequence comparisons of Dnd with other GTPases showed strongest homology to Arl3 GTPases. Dnd appears to be a functional GTPase based on sequence identity in critical residues, and this is bolstered by functional data. GTPases have a conserved threonine at residue 31 that binds GTP and is required for enzymatic function. When a T31N mutation was generated in *dnd*, this altered protein was unable to induce an S2 cell stellate phenotype and rescued *dnd* mutants poorly compared to wild-type. Similarly, the glutamine at residue 71 is conserved in GTPases and is required for GTP hydrolysis. Mutation of this residue in other GTPases results in a constitutively active GTPase. Alteration of Dnd Q71 to L71 resulted in a GTPase that was able to efficiently transform S2 cells to a stellate morphology, and also resulted in detectable, although rare, ectopic fusion of tracheal branches. These results strongly indicated that *dnd* encodes a functional Arl3 GTPase. Dnd also has glycine at residue 2, which in other GTPases is required for myristoylation and membrane localization. However, when G2 was mutated to alanine, S2 cell transformation and rescue of the *dnd* mutant phenotype were similar to wild-type *dnd*, suggesting that Dnd G2 is not essential for myristoylation or other key functions in the cell types tested. Similarly, human Arl3 has G2, but no evidence for myristoylation was found (Cavenagh et al., 1994; Kahn et al., 2006).

Vertebrate *Arl3* has been analyzed biochemically and genetically. Human *Arl3* is expressed in all tissues tested, although levels vary in different cell types (Cavenagh et al.,

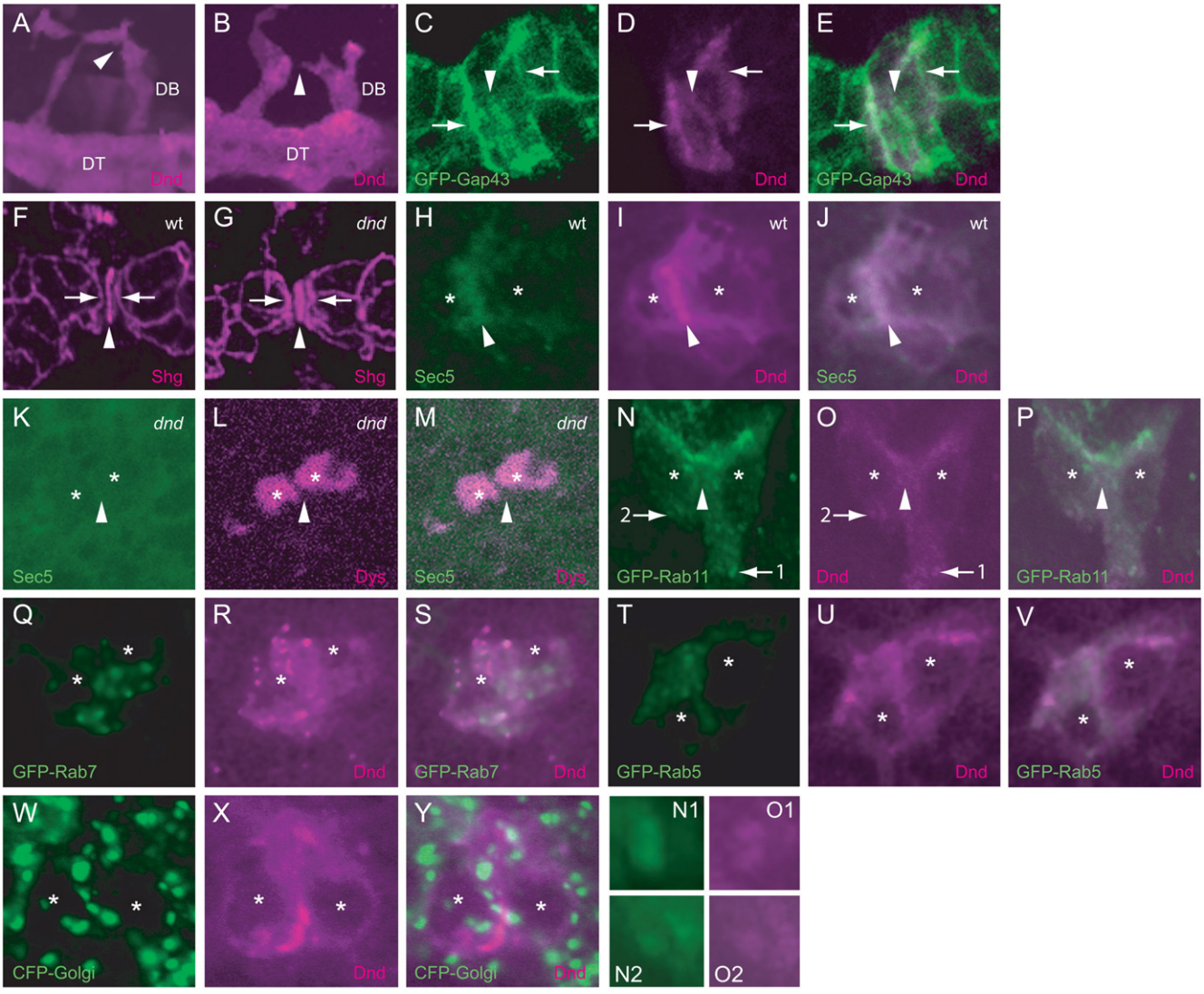

Fig. 7. Dnd control of exocyst function and vesicle trafficking in fusion cells. (A, B) Two segments of *btl-Gal4 UAS-dndQ71L* stage 15 embryos showing ectopic fusion (arrowheads) of DB. Embryos were stained with anti-Dnd (magenta). (C–E) Embryo with *btl-Gal4 UAS-GFP-Gap43* stained with anti-GFP and anti-Dnd. The outline (arrows) and site of fusion (arrowheads) of the doughnut-shaped fusion cells were seen with membrane-localized GFP-Gap43. Dnd is localized to the cytoplasm and membrane, including the site of fusion and cortical regions. (F, G) Wild-type (F) and *dnd* mutant (G) DT showing that Shg accumulates at the site of fusion (arrowheads) and junctions between fusion cells and their adjacent cells (arrows). This indicates that Shg accumulation is not dependent on *dnd* in DT. (H–J) Wild-type (wt) DT stained for (H, J) Sec5 and (I, J) Dnd showing that both Sec5 and Dnd are concentrated around the site of fusion (arrowhead). (*) indicates fusion cell nuclei. (K–M) *dnd* mutant DT stained for Sec5 (K) showing that Sec5 accumulation at the fusion site (arrowhead) requires *dnd* function. Dys (L, M) shows localization of the fusion cell nuclei. (N–P) Wild-type embryo with *btl-Gal4 UAS-GFP-Rab11* showing overlap (P) of some GFP^+ $Rab11^+$ recycling endosomal vesicles (N) with Dnd^+ vesicles (O). Some vesicles accumulate at the fusion site (arrowhead). The numbered arrows point to two locations containing Dnd^+ $Rab11^+$ vesicles that are shown at higher magnification in panels N1,O1 and N2,O2 at bottom. (Q–Y) Embryos with either (Q–R) *btl-Gal4 UAS-GFP-Rab7*, (T–V) *btl-Gal4 UAS-GFP-Rab5*, or (W–Y) *btl-Gal4 UAS-CFP-Golgi* showing that Dnd^+ vesicles do not substantially overlap with $Rab7^+$ late endosomal vesicles, $Rab5^+$ early endosomal vesicles, or Golgi.

1994). Considerable attention has been focused on the role of mammalian *Arl3* in photoreceptor cells. Human *Arl3* was shown to bind Retinitis pigmentosa 2 protein (RP2) in the presence of GTP (Bartolini et al., 2002). Mutations in human *RP2* lead to degeneration of photoreceptor cells (Breuer et al., 2002; Hardcastle et al., 1999; Schwahn et al., 1998). Arl3 is associated with microtubules, and since RP2 is membrane-bound, Arl3 may link the cytoskeleton to the membrane for photoreceptor vesicle trafficking or signaling (Grayson et al., 2002). Mammalian Arl3 was also shown to be associated with a number of microtubular structures, including centrosomes and mitotic spindles (Zhou et al., 2006). Reducing *Arl3* function with siRNA resulted in defects in cytokinesis, tubulin modification, and cell morphology. Arl3 also localized to the Golgi, and fragmentation of the Golgi was observed when *Arl3* levels were reduced. *Arl3* knockout mice were stunted, and showed defects in tubular organs, including the kidney, liver, and pancreas, as well as photoreceptor abnormalities (Schrick et al., 2006). One interpretation of the knockout mouse phenotypes was that the *Arl3* mutant is defective in membrane transport of proteins important for the functions of each cell type affected. While the roles of mammalian Arl3

appear to be diverse, common themes include localization to microtubules, potential roles in vesicle transport to the membrane, and defects in tubular organs. In these regards, the *Drosophila dnd* and mammalian Arl3 genes share functional similarity.

Dnd controls membrane trafficking of vesicles

Both cell culture and in vivo experiments support a role for Dnd in controlling the transport of vesicles to the membrane. The cell culture experiments revealed that Dnd is associated with actin-containing particles that traffic along actin/microtubule-rich processes. The particles also contain Sec5 and Rab11, suggesting that they are destined for export to the membrane. However, the nature of these particles and the significance of their $Sec5^+$ and $Rab11^+$ localization are currently unknown. Nevertheless, the association of Dnd^+ $Sec5^+$ $Rab11^+$ particles with actin/microtubule-containing processes in *dndQ71L* stellate cells, suggested that Dnd might control fusion cell vesicle trafficking. Further analyses in tracheal fusion cells revealed that Dnd was localized to $Sec5^+$ vesicles, and these vesicles accumulated around the site of fusion. Furthermore, Sec5 localization was absent in *dnd* mutant fusion cells. This result could be interpreted in several ways including: (1) Dnd is required for association of the exocyst with secretory vesicles, (2) the association of secretory vesicles with microtubules requires Dnd, and (3) trafficking of vesicles to the membrane requires Dnd. Some Dnd^+ vesicles also overlap with Rab11, but not significantly with Rab5, Rab7, or Golgi. This indicates that some of the Dnd^+ vesicles may be recycling endosomes, and Dnd-mediated membrane transport may include recycled membrane proteins, as well as proteins derived from the Golgi. Since the Dnd^+ $Sec5^+$ vesicles tend to accumulate near the fusion site, the transport is directed to specific sites within the cell.

Dnd directs reorganization of the cytoskeleton and cell shape

When S2 cells expressed *dndQ71L*, 40% of the cells took on a stellate morphology. These cells lost cortical actin and their lamella, and, instead, had long actin/microtubule processes with prominent particles attached. Similar S2 cell morphology has been previously observed by disrupting the actin filament network with cytochalasin D or reducing Arp2/3 levels (Kural et al., 2005; Rogers et al., 2003). One current model for how con A-treated S2 cells form a lamella begins with con A stimulating an unknown cell surface receptor (Rogers et al., 2003). The receptor stimulates the Rac and Mtl GTPases and the Nck SH2–SH3 adaptor protein. These proteins activate SCAR, which binds Arp2/3, leading to actin polymerization and lamella formation. In contrast, activated Dnd results in loss of F-actin, and could be enhancing actin depolymerization or inhibiting polymerization. F-actin is thought to inhibit the extension of microtubule-containing processes to the membrane. Thus, *dndQ71L*-transformed cells result in loss of F-actin, allowing the actin/microtubule-containing processes to extend from the cell body. Another GTPase, mammalian RalA, was shown to both control actin cytoskeletal remodeling, as well as interact with the exocyst (Sugihara et al., 2002), indicating that GTPases may play prominent roles in coordinating cytoskeletal organization with secretion.

How does the Dnd actin-destabilizing activity observed in S2 cells correlate with potential functions in fusion cells? There are several possibilities. During exocytotic vesicle transport, the vesicles migrate toward the membrane along microtubules. However, it is thought that they must leave the microtubules and transit through cortical actin to reach the membrane. In essence, microtubules are employed for long-range transport, and F-actin for short-range transport (Goode et al., 2000; Wang and Hsu, 2006). Consequently, Dnd, in addition to its role in mediating vesicle transport along microtubules, may regulate the local polymerization state of cortical actin allowing the vesicles to fuse with the membrane.

When fusion cells meet, Shg recruits Short stop to contact sites and promotes assembly of the F-actin/microtubule-containing fusion track (Lee et al., 2003). Membrane formation subsequently occurs along the fusion track. Later as lumenal fusion occurs between the two fusion cells, disassembly of some cytoskeletal elements may be required (Lee et al., 2003). Thus, Dnd's ability to affect F-actin depolymerization may be required for a cytoskeletal disassembly step during lumen formation, in addition to a possible role in trafficking of vesicles to the membrane.

Conclusions

This paper proposes at least two functions of *dnd* in fusion cells. One is involved in controlling actin polymerization and the other with vesicle transport to the membrane. These two functions could be connected. The work on *Drosophila dnd* shares similarities with the work on vertebrate Arl3, which affects formation of tubular structures, binds to microtubules, and may influence membrane transport. While the data support a role for *dnd* in lumenal fusion, many questions remain. What cargoes are being delivered to the membrane? One possible candidate, Shg, seems unlikely, although it cannot be ruled-out that some Shg is delivered by Dnd^+ vesicles to specific fusion cell locations. Since Shg is a cargo of the exocyst in thoracic epithelial cells (Langevin et al., 2005), why is it not transported by the exocyst in fusion cells? One possibility is that exocyst subunit heterogeneity may occur between fusion cells and other cell types, allowing different cargoes to be transported (Mehta et al., 2005). Other possibilities for the function of the fusion cell exocyst and Dnd are trafficking lumenal membrane proteins and mediating intracellular membrane fusion events that govern cell shape changes. Assuming that the Dnd effect on actin polymerization observed in S2 cells has a fusion cell correlate, which fusion cell F-actin filaments are affected by Dnd? One possibility is cortical actin that is involved in vesicle transport. In this regard, does Dnd influence the activity of the SCAR/Arp2/3 complex or cofilin, both which control actin polymerization? Alternatively, does Dnd affect the F-actin found in the developing fusion track? What are the relative contributions of Dnd^+ recycling endosomal vesicles vs. direct transport of Dnd^+

vesicles from the Golgi to the membrane? Dnd is also expressed in sensory cells: what is its role in these cells?

Acknowledgments

The authors would like to thank Don Ready, Greg Rogers, Nasser Rusan, and Tom Schwarz for advice and reagents. We would also like to acknowledge the importance of reagents from the Developmental Studies Hybridoma Bank (University of Iowa), the Bloomington *Drosophila* Stock Center, and Berkeley *Drosophila* Genome Project. This work was supported by grants from NSF (IBN-0316102; Developmental Mechanisms) and the National Center for Research Resources (National Institutes of Health) to STC, and by a March of Dimes Basil O'Connor Starter Scholar Research Award to SLR.

Appendix A. Supplementary data

Supplementary data associated with this article can be found, in the online version, at doi:10.1016/j.ydbio.2007.08.049.

References

Bartolini, F., Bhamidipati, A., Thomas, S., Schwahn, U., Lewis, S.A., Cowan, N.J., 2002. Functional overlap between retinitis pigmentosa 2 protein and the tubulin-specific chaperone cofactor C. J. Biol. Chem. 277, 14629–14634.

Brand, A.H., Perrimon, N., 1993. Targeted gene expression as a means of altering cell fates and generating dominant phenotypes. Development 118, 401–415.

Breuer, D.K., Yashar, B.M., Filippova, E., Hiriyanna, S., Lyons, R.H., Mears, A.J., Asaye, B., Acar, C., Vervoort, R., Wright, A.F., Musarella, M.A., Wheeler, P., MacDonald, I., Iannaccone, A., Birch, D., Hoffman, D.R., Fishman, G.A., Heckenlively, J.R., Jacobson, S.G., Sieving, P.A., Swaroop, A., 2002. A comprehensive mutation analysis of RP2 and RPGR in a North American cohort of families with X-linked retinitis pigmentosa. Am. J. Hum. Genet. 70, 1545–1554.

Cavenagh, M.M., Breiner, M., Schurmann, A., Rosenwald, A.G., Terui, T., Zhang, C., Randazzo, P.A., Adams, M., Joost, H.G., Kahn, R.A., 1994. ADP-ribosylation factor (ARF)-like 3, a new member of the ARF family of GTP-binding proteins cloned from human and rat tissues. J. Biol. Chem. 269, 18937–18942.

Entchev, E.V., Schwabedissen, A., Gonzalez-Gaitan, M., 2000. Gradient formation of the TGF-beta homolog Dpp. Cell 103, 981–991.

Goode, B.L., Drubin, D.G., Barnes, G., 2000. Functional cooperation between the microtubule and actin cytoskeletons. Curr. Opin. Cell Biol. 12, 63–71.

Grayson, C., Bartolini, F., Chapple, J.P., Willison, K.R., Bhamidipati, A., Lewis, S.A., Luthert, P.J., Hardcastle, A.J., Cowan, N.J., Cheetham, M.E., 2002. Localization in the human retina of the X-linked retinitis pigmentosa protein RP2, its homologue cofactor C and the RP2 interacting protein Arl3. Hum. Mol. Genet. 11, 3065–3074.

Hardcastle, A.J., Thiselton, D.L., Van Maldergem, L., Saha, B.K., Jay, M., Plant, C., Taylor, R., Bird, A.C., Bhattacharya, S., 1999. Mutations in the RP2 gene cause disease in 10% of families with familial X-linked retinitis pigmentosa assessed in this study. Am. J. Hum. Genet. 64, 1210–1215.

Hogan, B.L., Kolodziej, P.A., 2002. Organogenesis: molecular mechanisms of tubulogenesis. Nat. Rev., Genet. 3, 513–523.

Jiang, L., Crews, S.T., 2003. The *Drosophila* dysfusion basic helix–loop–helix (bHLH)-PAS gene controls tracheal fusion and levels of the trachealess bHLH-PAS protein. Mol. Cell. Biol. 23, 5625–5637.

Jiang, L., Crews, S.T., 2006. Dysfusion transcriptional control of *Drosophila* tracheal migration, adhesion, and fusion. Mol. Cell. Biol. 26, 6547–6556.

Kahn, R.A., Cherfils, J., Elias, M., Lovering, R.C., Munro, S., Schurmann, A., 2006. Nomenclature for the human Arf family of GTP-binding proteins: ARF, ARL, and SAR proteins. J. Cell Biol. 172, 645–650.

Kural, C., Kim, H., Syed, S., Goshima, G., Gelfand, V.I., Selvin, P.R., 2005. Kinesin and dynein move a peroxisome in vivo: a tug-of-war or coordinated movement? Science 308, 1469–1472.

Langevin, J., Morgan, M.J., Sibarita, J.B., Aresta, S., Murthy, M., Schwarz, T., Camonis, J., Bellaiche, Y., 2005. *Drosophila* exocyst components Sec5, Sec6, and Sec15 regulate DE-Cadherin trafficking from recycling endosomes to the plasma membrane. Dev. Cell 9, 355–376.

Lee, S., Kolodziej, P.A., 2002. The plakin Short Stop and the RhoA GTPase are required for E-cadherin-dependent apical surface remodeling during tracheal tube fusion. Development 129, 1509–1520.

Lee, M., Lee, S., Zadeh, A.D., Kolodziej, P.A., 2003. Distinct sites in E-cadherin regulate different steps in *Drosophila* tracheal tube fusion. Development 130, 5989–5999.

Li, B.X., Satoh, A.K., Ready, D.F., 2007. Myosin V, Rab11, and dRip11 direct apical secretion and cellular morphogenesis in developing *Drosophila* photoreceptors. J. Cell Biol. 177, 659–669.

Linari, M., Hanzal-Bayer, M., Becker, J., 1999. The delta subunit of rod specific cyclic GMP phosphodiesterase, PDE delta, interacts with the Arf-like protein Arl3 in a GTP specific manner. FEBS Lett. 458, 55–59.

Manning, G., Krasnow, M.A., 1993. Development of the *Drosophila* tracheal system. In: Bate, M., Martinez Arias, A. (Eds.), The Development of *Drosophila melanogaster*. Cold Spring Harbor Laboratory Press, Cold Spring Harbor, NY, pp. 609–685.

Mehta, S.Q., Hiesinger, P.R., Beronja, S., Zhai, R.G., Schulze, K.L., Verstreken, P., Cao, Y., Zhou, Y., Tepass, U., Crair, M.C., Bellen, H.J., 2005. Mutations in *Drosophila* sec15 reveal a function in neuronal targeting for a subset of exocyst components. Neuron 46, 219–232.

Murthy, M., Schwarz, T.L., 2004. The exocyst component Sec5 is required for membrane traffic and polarity in the *Drosophila* ovary. Development 131, 377–388.

Murthy, M., Garza, D., Scheller, R.H., Schwarz, T.L., 2003. Mutations in the exocyst component Sec5 disrupt neuronal membrane traffic, but neurotransmitter release persists. Neuron 37, 433–447.

Patel, N.H., Snow, P.M., Goodman, C.S., 1987. Characterization and cloning of fasciclin III: a glycoprotein expressed on a subset of neurons and axon pathways in *Drosophila*. Cell 48, 975–988.

Rogers, S.L., Wiedemann, U., Stuurman, N., Vale, R.D., 2003. Molecular requirements for actin-based lamella formation in *Drosophila* S2 cells. J. Cell Biol. 162, 1079–1088.

Samakovlis, C., Hacohen, N., Manning, G., Sutherland, D., Guillemin, K., Krasnow, M.A., 1996a. Development of the *Drosophila* tracheal system occurs by a series of morphologically distinct but genetically coupled branching events. Development 122, 1395–1407.

Samakovlis, C., Manning, G., Steneberg, P., Hacohen, N., Cantera, R., Krasnow, M.A., 1996b. Genetic control of epithelial tube fusion during *Drosophila* tracheal development. Development 122, 3531–3536.

Satoh, A.K., O'Tousa, J.E., Ozaki, K., Ready, D.F., 2005. Rab11 mediates post-Golgi trafficking of rhodopsin to the photosensitive apical membrane of *Drosophila* photoreceptors. Development 132, 1487–1497.

Schrick, J.J., Vogel, P., Abuin, A., Hampton, B., Rice, D.S., 2006. ADP-ribosylation factor-like 3 is involved in kidney and photoreceptor development. Am. J. Pathol. 168, 1288–1298.

Schwahn, U., Lenzner, S., Dong, J., Feil, S., Hinzmann, B., van Duijnhoven, G., Kirschner, R., Hemberger, M., Bergen, A.A., Rosenberg, T., Pinckers, A.J., Fundele, R., Rosenthal, A., Cremers, F.P., Ropers, H.H., Berger, W., 1998. Positional cloning of the gene for X-linked retinitis pigmentosa 2. Nat. Genet. 19, 327–332.

Shimizu, H., Kawamura, S., Ozaki, K., 2003. An essential role of Rab5 in uniformity of synaptic vesicle size. J. Cell Sci. 116, 3583–3590.

Sommer, B., Oprins, A., Rabouille, C., Munro, S., 2005. The exocyst component Sec5 is present on endocytic vesicles in the oocyte of *Drosophila melanogaster*. J. Cell Biol. 169, 953–963.

Stewart, B.A., Atwood, H.L., Renger, J.J., Wang, J., Wu, C.F., 1994. Improved stability of *Drosophila* larval neuromuscular preparations in haemolymph-like physiological solutions. J. Comp. Physiol., A 175, 179–191.

Sugihara, K., Asano, S., Tanaka, K., Iwamatsu, A., Okawa, K., Ohta, Y., 2002. The exocyst complex binds the small GTPase RalA to mediate filopodia formation. Nat. Cell Biol. 4, 73–78.

Tanaka-Matakatsu, M., Uemura, T., Oda, H., Takeichi, M., Hayashi, S., 1996. Cadherin-mediated cell adhesion and cell motility in *Drosophila* trachea regulated by the transcription factor Escargot. Development 122, 3697–3705.

Tomancak, P., Beaton, A., Weiszmann, R., Kwan, E., Shu, S., Lewis, S.E., Richards, S., Ashburner, M., Hartenstein, V., Celniker, S.E., Rubin, G.M., 2002. Systematic determination of patterns of gene expression during *Drosophila* embryogenesis. Genome Biol, research0088. 1–088.14.

Wang, S., Hsu, S.C., 2006. The molecular mechanisms of the mammalian exocyst complex in exocytosis. Biochem. Soc. Trans. 34, 687–690.

Zhou, C., Cunningham, L., Marcus, A.I., Li, Y., Kahn, R.A., 2006. Arl2 and Arl3 regulate different microtubule-dependent processes. Mol. Biol. Cell 17, 2476–2487.